ANNALS of PHYSICS

Solution of Dirac equation and greybody radiation around a regular Bardeen black hole surrounded by quintessence

Ahmad Al-Badawi [a],*, İzzet Sakallı [b], Sara Kanzi [b]

[a] *Department of Physics, Al-Hussein Bin Talal University, P. O. Box: 20, 71111, Ma'an, Jordan*
[b] *Physics Department, Arts and Sciences Faculty, Eastern Mediterranean University, Famagusta, North Cyprus via Mersin 10, Turkey*

A R T I C L E   I N F O

A B S T R A C T

The exact solutions of the Dirac equation that describe a massive, non-charged particle with spin$-\frac{1}{2}$ in the curved spacetime geometry of regular Bardeen black hole surrounded by quintessence (BBHSQ) are investigated. We first derive the Dirac equation in the BBHSQ background using a null tetrad in the Newman–Penrose formalism. Afterwards, we separate the Dirac equation into ordinary differential equations for the radial and angular parts. The angular equations are solved exactly in terms of standard spherical harmonics. The radial part equations are transformed into one-dimensional Schrödinger like wave equations with effective potentials. The effect of the quintessence on the regular Bardeen black hole is analyzed via the physical behaviors of the effective potentials. We also exhibit the potential graphs by changing the quintessence parameters, magnetic monopole charge parameter, and the frequency of the particle in the physically acceptable regions. Finally, we study the greybody factors of bosons and fermions from the BBHSQ.

© 2019 Elsevier Inc. All rights reserved.

1. Introduction

At astrophysics scale, observations confirm the accelerating expansion of the universe [1]. To explain the expansion, it is suggested that the matter content in the universe has a negative pressure

---

called dark energy [2]. There are two kinds of negative pressure, first the cosmological constant [3,4] and the second is the so-called quintessence that causes the acceleration of the universe [5–7]. Quintessence is characterized by the state equation: $p = w_q \rho_q$ where p is the pressure, ρ_q is the energy density, and w_q is the state parameter. In addition, the scalar fields are also hypothetical forms of dark energy where a broad types of scalar field models have been suggested such as quintessence [8–15], phantom models [16–20], K-essence [21,22], quintom [23,24], and so on. Ultimately, the difference between these models is due to the magnitude of w_q and for quintessence $-1 \leq w_q \leq -\frac{1}{3}$. The quintessence model refers to a minimally coupled scalar field with a potential which decreases as the field increases. Quintessence is a scalar field with an equation of state where w_q is given by the potential energy and a kinetic term. Hence, quintessence is dynamic and generally has a density, and w_q parameter varies with time. By contrast, a cosmological constant is static, possessing a fixed energy density, and it has $w_q = -1$.

Usually, black holes (BHs) have singularity inside the horizon. However, Bardeen BH (BBH) is a regular BH which does not have singularity inside the horizon. It was first introduced by Bardeen [25]. Since Bardeen introduced his model, many other models of spherical symmetric regular BHs were presented in the literature [26–36]. Later, in Ref. [37,38] the authors have shown that BBH model is explained as the gravitational field produced by a nonlinear magnetic monopole. This explanation was extended so that it includes nonlinear electric charge. Moreover, regular BHs surrounded by quintessence have received major attention. Kiselev [8] obtained the first analytical solutions with spherical symmetry with quintessence surrounding the static BHs. Later, the generalization of Kiselev solutions was obtained by constructing their rotating counterpart [39,40]. On the other hand, the effect of quintessence on BHs has received considerable attention and their thermodynamics has been investigated. For example, in Ref. [41] the thermodynamic properties of the Bardeen black hole surrounded by quintessence (BBHSQ) was thoroughly studied.

In this paper, we consider the Dirac equation in regular BBHSQ space–time. Recall that analytical solutions to the Dirac equation can be obtained in several backgrounds [42–48]. A reader is referred to see the complete analytical solutions to the Dirac equation on de-Sitter and anti de-Sitter space–time [49–53]. The Dirac equation that we consider in this study describes a massive and non-charged particle with spin-$\frac{1}{2}$. To this end, we choose a null tetrad in order to apply the Newman-Penrose (NP) formalism. Next, we separate the Dirac equation into ordinary differential equations and the get coupled radial and angular parts. The angular part equations are solved exactly in terms of standard spherical harmonics. The radial equations are transformed into one dimensional Schrödinger like differential wave equations with effective potentials. In addition, we investigate the behavior of the effective potentials by plotting them as a function of radial distance and expose the effect of the quintessence parameters, magnetic monopole charge parameter, and the frequency of the particle on them. Finally, we study the outcome of scattering a wave off a BBHSQ in terms of an absorption cross-section. The absorption cross-section, which is a measure for the probability of an absorption process, is directly connected to the greybody factor. Then, we compute the greybody factor, which is nothing but the transmission probability for an outgoing wave emitted from the event horizon of the BBHSQ to reach the asymptotic region [54–57]. Our main motivation in the present paper paves the way to study the quasi-normal modes associated to a field of spin-$\frac{1}{2}$ on the BBHSQ background. Further, the given analytical expressions of the solution could be useful for the study of the thermodynamical properties of the spinor field in same background.

The plan of the paper is as follows. In the next section, we give a brief discussion on the regular BBHSQ space–time. In Section 3, we present the Dirac equation in BBHSQ geometry and decouple the equations into ordinary differential equations for having the radial and angular parts. We then obtain solutions of the angular and radial equations in Section 4. The influence of the quintessence parameter is investigated through the behavior of the effective potentials by plotting them as a function of radial distance in the physically acceptable region. Sections 5 and 6 are devoted to the studies of greybody factors of the BBHSQ for the spin-0 and spin-$\frac{1}{2}$ particles, respectively. Finally, we present our conclusions in Section 7.

2. Regular BBHSQ space–time

In this section, we shall give a brief introduction to BBHSQ which was obtained by Kiselev [8], who assumed a spherically symmetric static gravitational field with the following energy–momentum tensor:

$$T_t^t = T_r^r = \rho_q,$$
$$T_\theta^\theta = T_\phi^\phi = -\frac{\rho_q}{2}\left(3w_q + 1\right), \tag{1}$$

where w_q is the quintessence state parameter with range $-1 \leq w_q \leq -1/3$ and ρ_q is the density of the quintessence matter given by

$$\rho_q = -\frac{3cw_q}{2r^{3(1+w_q)}}, \tag{2}$$

where c is the positive normalization factor ($c \geq 0$). The metric of the regular BBHSQ can be expressed as [41]

$$ds^2 = -f(r)\, dt^2 + f^{-1}(r) dr^2 + r^2\left(d\theta^2 + \sin^2\theta d\phi^2\right) \tag{3}$$

where $f(r)$ has the following form

$$f(r) = 1 - \frac{2Mr^2}{\left(r^2 + \beta^2\right)^{3/2}} - \frac{c}{r^{3w_q+1}}. \tag{4}$$

in which M is the mass of the BH and β can represent the monopole charge of a self-gravitating magnetic field described by a nonlinear electrodynamics source or an electric source with a field that does not behave as the Coulomb field [58]. In fact, c term is related to the density of quintessence:

$$\rho_q = \frac{-3cw_q}{2r^{3(w_q+1)}}.$$

The curvature of the metric (3) has the form of

$$R = 2T_\mu^\mu = 2\rho_q\left(3w_q - 1\right), \tag{5}$$

which admits a singularity at $r = 0$ if $w_q \neq \{0, \frac{1}{3}, -1\}$. Therefore, the metric in (3) represents a spherically symmetric solutions for the Einstein equations describing BBHSQ with the energy–momentum tensors given in (1). This metric satisfies all the required limits: when ($c = 0 = \beta$), we have Schwarzschild BH metric; as ($c = 0, \beta \neq 0$), we get Bardeen BH; and ($c \neq 0, \beta \neq 0$) yields the BBHSQ.

We use the NP formalism [59,60] to write and solve the Dirac equation in the spacetime of (3). Therefore let us define the complex null tetrad vectors ($l, n, m, \overline{m}$) for the metric (3) where they satisfy the orthogonality conditions, ($l.n = -m.\overline{m} = 1$) as

$$l_\mu = dt - \frac{dr}{f(r)},$$
$$n_\mu = \frac{1}{2}f(r)\, dt + \frac{1}{2}dr,$$
$$m_\mu = \frac{-r}{\sqrt{2}}(d\theta + i\sin\theta d\phi),$$
$$\overline{m}_\mu = \frac{-r}{\sqrt{2}}(d\theta - i\sin\theta d\phi), \tag{6}$$

and

$$l^\mu = f(r)\, dt + dr,$$
$$n^\mu = \frac{1}{2}dt - \frac{1}{2}f(r)\, dr,$$

$$m^\mu = \frac{1}{\sqrt{2}r}\left(d\theta + \frac{i}{\sin\theta}d\phi\right),$$

$$\overline{m}^\mu = \frac{-r}{\sqrt{2}}(d\theta - i\sin\theta d\phi), \tag{7}$$

We determine the nonzero NP complex spin coefficients [60] as follows

$$\rho = -\frac{1}{r}, \qquad \mu = \frac{1}{2r} - \frac{Mr}{\left(r^2 + \beta^2\right)^{3/2}} - \frac{c}{2r^{3w_q+2}},$$

$$\gamma = \frac{Mr}{2}\left[\frac{r^2 - 2\beta^2}{\left(r^2 + \beta^2\right)^{5/2}}\right] + \frac{(3w+1)c}{4r^2r^{3w}}, \qquad \alpha = -\beta_1 = \frac{-\cot\theta}{2\sqrt{2}r}. \tag{8}$$

3. Dirac equation in BBHSQ

We write the Dirac equations in the NP formalism by using the standard notation for the spin coefficients [59,60] as

$$\left(l^\mu\partial_\mu + \epsilon - \rho\right)F_1 + \left(\overline{m}^\mu\partial_\mu + \pi - \alpha\right)F_2 = i\mu_0 G_1, \tag{9}$$

$$\left(n^\mu\partial_\mu + \mu - \gamma\right)F_2 + \left(m^\mu\partial_\mu + \beta_1 - \tau\right)F_1 = i\mu_0 G_2, \tag{10}$$

$$\left(l^\mu\partial_\mu + \overline{\epsilon} - \overline{\rho}\right)G_2 - \left(m^\mu\partial_\mu + \overline{\pi} - \overline{\alpha}\right)G_1 = i\mu_0 F_2, \tag{11}$$

$$\left(n^\mu\partial_\mu + \overline{\mu} - \overline{\gamma}\right)G_1 - \left(\overline{m}^\mu\partial_\mu + \overline{\beta}_1 - \overline{\tau}\right)G_2 = i\mu_0 F_1. \tag{12}$$

where F_1, F_2, G_1 and G_2 represent the components of the wave functions "Dirac spinors", the mass of the particle $\mu_0 = \sqrt{2}\mu_p$ and $\epsilon, \rho, \pi, \alpha, \mu, \gamma, \beta_1, \tau$ are the spin coefficients and bar over a quantity denotes complex conjugation. We now study the Dirac equations (9)–(12) in the background of metric (3). To solve the Dirac equations, we will consider the corresponding Compton wave of the Dirac particle as in the form of $F = F(r, \theta)e^{i(kt+m\phi)}$, where k is the frequency of the incoming wave and m is the azimuthal quantum number of the wave. For separable solutions, we assume [59],

$$rF_1 = R_1(r)A_1(\theta)\exp\left[i\left(kt + m\phi\right)\right],$$

$$F_2 = R_2(r)A_2(\theta)\exp\left[i\left(kt + m\phi\right)\right],$$

$$G_1 = R_2(r)A_1(\theta)\exp\left[i\left(kt + m\phi\right)\right],$$

$$rG_2 = R_1(r)A_2(\theta)\exp\left[i\left(kt + m\phi\right)\right]. \tag{13}$$

Substituting the appropriate spin coefficients (8) and the spinors (13) into the Dirac equations (9)–(12), we obtain the following set of equations

$$A_1\left(\frac{d}{dr} + i\frac{k}{f}\right)R_1 + \frac{1}{\sqrt{2}}R_2\mathbf{L}A_2 = i\mu_0 rR_2 A_1,$$

$$r^2 f A_2\left(\frac{d}{dr} - i\frac{k}{f} + \frac{2f + rf'}{2rf}\right)R_2 - \sqrt{2}R_1\mathbf{L}^\dagger A_1 = -2i\mu_0 rR_1 A_2,$$

$$A_2\left(\frac{d}{dr} + i\frac{k}{f}\right)R_1 - \frac{1}{\sqrt{2}}R_2\mathbf{L}^\dagger A_1 = i\mu_0 rR_2 A_2,$$

$$r^2 f A_1\left(\frac{d}{dr} - i\frac{k}{f} + \frac{2f + rf'}{2rf}\right)R_2 + \sqrt{2}R_1\mathbf{L}A_2 = -2i\mu_0 rR_1 A_1. \tag{14}$$

where $\mathbf{L}$ and $\mathbf{L}^\dagger$ are the angular operators, which are known as the laddering operators:

$$\mathbf{L} = \frac{d}{d\theta} + \frac{m}{\sin\theta} + \frac{\cot\theta}{2}, \qquad \mathbf{L}^\dagger = \left(\frac{d}{d\theta} - \frac{m}{\sin\theta} + \frac{\cot\theta}{2}\right) \tag{15}$$

From (14) and (15), we get

$$\left(\frac{d}{dr} + i\frac{k}{f}\right) R_1 - i\mu_0 r R_2 = -\lambda_1 R_2,$$

$$r^2 f \left(\frac{d}{dr} - i\frac{k}{f} + \frac{2f + rf'}{2rf}\right) R_2 + 2i\mu_0 r R_1 = \lambda_2 R_1,$$

$$\left(\frac{d}{dr} + i\frac{k}{f}\right) R_1 - i\mu_0 r R_2 = \lambda_3 R_2,$$

$$r^2 f \left(\frac{d}{dr} - i\frac{k}{f} + \frac{2f + rf'}{2rf}\right) R_2 + 2i\mu_0 r R_1 = -\lambda_4 R_1, \tag{16}$$

$$\mathbf{L}A_2 = \lambda_1 A_1, \qquad \mathbf{L}^\dagger A_1 = \lambda_2 A_2,$$

$$\mathbf{L}^\dagger A_1 = \lambda_3 A_2, \qquad \mathbf{L}A_2 = \lambda_4 A_1, \tag{17}$$

The constants λ_1, λ_2, λ_3, and λ_4 are called the separation constants. To obtain the radial and the angular pair equations, we assume ($\lambda_4 = \lambda_1 = -\lambda$, $\lambda_2 = \lambda_3 = \lambda$), therefore (16) and (17) reduce to

$$\left(\frac{d}{dr} + i\frac{k}{f}\right) R_1 = (\lambda + i\mu_0 r) R_2, \tag{18}$$

$$\left(\frac{d}{dr} - i\frac{k}{f} + \frac{2f + rf'}{2rf}\right) R_2 = \frac{1}{r^2 f} (\lambda - 2i\mu_0 r) R_1, \tag{19}$$

$$\mathbf{L}A_2 = -\lambda A_1, \qquad \mathbf{L}^\dagger A_1 = \lambda A_2. \tag{20}$$

4. Solution of angular and radial equations

Angular equations (20) can be rewritten as

$$\frac{dA_1}{d\theta} + \left(\frac{\cot\theta}{2} - \frac{m}{\sin\theta}\right) A_1 = -\lambda A_2, \tag{21}$$

$$\frac{dA_2}{d\theta} + \left(\frac{\cot\theta}{2} + \frac{m}{\sin\theta}\right) A_2 = \lambda A_1. \tag{22}$$

which lead to the spin-weighted spheroidal harmonics whose solution is given in terms of standard spherical harmonics [60–62] as

$$A_{1,2} = Y_l^m (\theta), \tag{23}$$

with $\lambda^2 = \left(l + \frac{1}{2}\right)^2$.

The radial equations (18) and (19) can be rearranged as

$$\left(\frac{d}{dr} + i\frac{k}{f}\right) R_1 = (\lambda + i\mu_* r) R_2, \tag{24}$$

$$r\sqrt{f} \left(\frac{d}{dr} - i\frac{k}{f} + \frac{2f + rf'}{2rf}\right) r\sqrt{f} R_2 = (\lambda - i\mu_* r) R_1, \tag{25}$$

where μ_* is the normalized rest mass of the spin-$\frac{1}{2}$ particle.

Our task now is to put the radial equations (24) and (25) in the form of one dimensional wave equations. To this end, we follow the method applied by Chandrasekhar's book [59]. We start by making the following transformations

$$P_1 = R_1, \qquad P_2 = r\sqrt{f} R_2. \tag{26}$$

Hence, (24) and (25) transform to

$$\frac{dP_1}{dr} + i\frac{k}{f} P_1 = \frac{1}{r^2 f} (\lambda + i\mu_* r) P_2, \tag{27}$$

$$\frac{dP_2}{dr} - i\frac{k}{f}P_2 + \frac{2f + rf'}{2rf}P_2 = \frac{1}{r^2 f}\left(\lambda - i\mu_* r\right)P_1, \tag{28}$$

Assuming

$$\frac{du}{dr} = \frac{1}{f}, \tag{29}$$

then, (27) and (28), in terms of the new independent variable u, become

$$\frac{dP_1}{du} + ikP_1 = \frac{\sqrt{f}}{r}\left(\lambda + i\mu_* r\right)P_2, \tag{30}$$

$$\frac{dP_2}{du} - ikP_2 + \frac{2f + rf'}{2rf}P_2 = \frac{\sqrt{f}}{r}\left(\lambda - i\mu_* r\right)P_1. \tag{31}$$

where

$$u = r - \sqrt{M^2 - a^2 M^2 - 2Mr}\,\tan^{-1}\left(\frac{r}{\sqrt{M^2 - a^2 M^2 - 2Mr}}\right). \tag{32}$$

Let us apply another transformation:

$$P_1 = \phi_1 \exp\left[\frac{-i}{2}\tan^{-1}\left(\frac{\mu_* r}{\lambda}\right)\right], \qquad P_2 = \phi_2 \exp\left[\frac{i}{2}\tan^{-1}\left(\frac{\mu_* r}{\lambda}\right)\right], \tag{33}$$

and then changing the variable u into $\widehat{r}$ as $\widehat{r} = u - \frac{1}{2k}\tan^{-1}\left(\frac{\mu_0 r}{\lambda}\right)$, then (30) and (31) can be written in the alternative forms:

$$\frac{d\phi_1}{d\widehat{r}} + ik\phi_1 = W\phi_2, \tag{34}$$

$$\frac{d\phi_2}{d\widehat{r}} - ik\phi_2 = W\phi_1, \tag{35}$$

where

$$W = \frac{2k\sqrt{f}\left(\lambda^2 + \mu_*^2 r^2\right)^{3/2}}{2kr\left(\lambda^2 + \mu_*^2 r^2\right) + rf\lambda\mu_*}. \tag{36}$$

To put (34) and (35) into one dimensional wave equations, we define

$$2\phi_1 = \psi_1 + \psi_2, \qquad 2\phi_2 = \psi_1 - \psi_2. \tag{37}$$

Hence, (34) and (35) become

$$\frac{d\psi_1}{d\widehat{r}} - W\psi_1 = -ik\psi_2, \tag{38}$$

$$\frac{d\psi_2}{d\widehat{r}} + W\psi_2 = -ik\psi_1. \tag{39}$$

Finally, we end up with the following pair of one dimensional wave equations

$$\frac{d^2\psi_1}{d\widehat{r}^2} + k^2\psi_1 = V_+\psi_1, \tag{40}$$

$$\frac{d^2\psi_2}{d\widehat{r}^2} + k^2\psi_2 = V_-\psi_2, \tag{41}$$

where the effective potentials can be obtained from

$$V_\pm = W^2 \pm \frac{dW}{d\widehat{r}}. \tag{42}$$

We calculate the effective potentials as

$$V_\pm = \frac{r^2 B^3}{D^2}\left(1 - \frac{2Mr^2}{(r^2+\beta^2)^{3/2}} - \frac{c}{r^{3w_q+1}}\right)$$
$$\pm \frac{r}{D^2}\sqrt{B^3 - \frac{2Mr^2 B^3}{(r^2+\beta^2)^{3/2}} - \frac{cB^3}{r^{3w_q+1}}}\left((r-M)B + 3r^3\mu_*^2 - \frac{6r^5\mu_*^2 M}{(r^2+\beta^2)^{3/2}} - \frac{3r^3\mu_*^2 c}{r^{3w_q+1}}\right)$$
$$\mp \frac{r^3 B^{5/2}}{D^3}\left(1 - \frac{2Mr^2}{(r^2+\beta^2)^{3/2}} - \frac{c}{r^{3w_q+1}}\right)^{3/2}\left[(2rB + 2r^3\mu_*^2) + \frac{(r-M)\lambda\mu_*}{k}\right], \tag{43}$$

where

$$B = (\lambda^2 + \mu_*^2 r^2), \qquad D = r^2 B + \frac{\lambda\mu_* r^2}{2k}\left(1 - \frac{2Mr^2}{(r^2+\beta^2)^{3/2}} - \frac{c}{r^{3w_q+1}}\right). \tag{44}$$

Let us note that the effective potentials for the case of massless Dirac particle (neutrino) can be obtained by setting $\mu_* = 0$ in (43) namely

$$V_\pm = \lambda^2\left(\frac{1}{r^2} - \frac{2M}{(r^2+\beta^2)^{3/2}} - \frac{c}{r^{3w_q+3}}\right) \pm \frac{\lambda(r-M)}{r^3}\sqrt{\left(1 - \frac{2Mr^2}{(r^2+\beta^2)^{3/2}} - \frac{c}{r^{3w_q+1}}\right)}$$
$$\mp \frac{2\lambda}{r^2}\left(1 - \frac{2Mr^2}{(r^2+\beta^2)^{3/2}} - \frac{c}{r^{3w_q+1}}\right)^{3/2}, \tag{45}$$

whereas substituting $c = 0$, $\beta \neq 0$ reduces to the effective potentials for BBH

$$V_\pm = \frac{r^2 B^3}{D^2}\left(1 - \frac{2Mr^2}{(r^2+\beta^2)^{3/2}}\right)$$
$$\pm \frac{r}{D^2}\sqrt{B^3 - \frac{2Mr^2 B^3}{(r^2+\beta^2)^{3/2}}}\left((r-M)B + 3r^3\mu_*^2 - \frac{6r^5\mu_*^2 M}{(r^2+\beta^2)^{3/2}}\right)$$
$$\mp \frac{r^3 B^{5/2}}{D^3}\left(1 - \frac{2Mr^2}{(r^2+\beta^2)^{3/2}}\right)^{3/2}\left[(2rB + 2r^3\mu_*^2) + \frac{(r-M)\lambda\mu_*}{k}\right], \tag{46}$$

where

$$B = (\lambda^2 + \mu_*^2 r^2), \qquad D = r^2 B + \frac{\lambda\mu_* r^2}{2k}\left(1 - \frac{2Mr^2}{(r^2+\beta^2)^{3/2}}\right). \tag{47}$$

The complete solution of (40) and (41) can be obtained by the WKB approximation method (for more details, a reader is referred to [63,64]). To study the asymptotic behavior of the potentials (43), we can expand it up to order $O\left(\frac{1}{r}\right)^3$. The potentials (43) for BBHSQ (here, we choose $w_q = -\frac{1}{3}$) behave as

$$V_\pm \simeq \mu_*^2(1-c) - \frac{2M\mu_*^2 \pm \mu_* c\sqrt{1-c}}{r} + \eta_\pm\left(\frac{1}{r}\right)^2 + O\left(\frac{1}{r}\right)^3, \tag{48}$$

where

$$\eta_\pm = \left[\lambda^2(1-c) - \frac{\lambda\mu_*}{k}(c^2 - 2c + 1) \pm \frac{M\mu_*(3c \mp 4)}{\sqrt{1-c}} \pm 5M\mu_*\sqrt{1-c}\right], \tag{49}$$
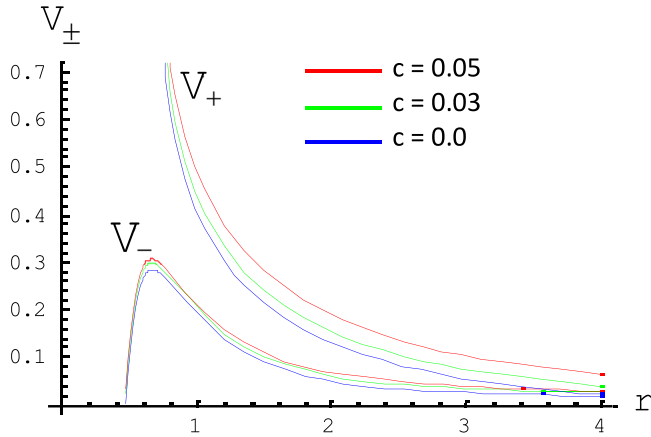
Fig. 1. Family of potential graphs $V_\pm$ for different values of c with $\mu^* = 0.12$, $k = 0.2$, $M = 0.5$, $\lambda = 1$, $\beta = 0.25$, and $w_q = -\frac{5}{6}$.

In case of neutrino, the potentials simplified to

$$V_\pm \simeq \lambda^2 \left(\frac{1}{r}\right)^2 + O\left(\frac{1}{r}\right)^3. \tag{50}$$

The first term in (48) represents the constant value of the potential at the asymptotic infinity. The second term corresponds to the monopole type potential, while the third term represents the dipole type potential. As seen from the asymptotic expansion of the potentials (48), the effect of adding the quintessence term $\left(\frac{c}{r^{3w_q+1}}\right)$ to the lapse function $f(r)$ in the metric (3) is observed at all terms. From (43), we notice that the potentials $V_\pm$ depend on the c, β, and k parameters. We would like to remind that the effect of the quintessence on BH has received considerable attention in General Relativity [65,66]. Therefore, it is interesting to investigate the quintessence affect the massive and non-charged Dirac particle.

It is obvious from (43) that the potentials become singular when $D = 0$. They also have local extrema when $(dV_\pm/dr) = 0$, however, these local extrema are very complicated algebraic equation to be solved. To understand the physical behavior of the potentials (43) in the physical region and to expose the effect of the quintessence parameters c, magnetic monopole charge parameter β and the frequency k of the particle, we make two-dimensional and three-dimensional plots of the potentials for massive particles. In all plots, we choose the fermion's mass $\mu_* = 0.12$ and the frequency $k = 0.2$ such that $k > \mu_*$. The effective potential $V_\pm$(43) versus r for different values of c is depicted in Fig. 1. It is observed that the potentials have sharp peaks for all values of c. We notice that when the normalization factor c increases, the sharpness of the potential peaks also increases. We deduce From Fig. 1 that, a massive Dirac particle in the presence of quintessence matter ($c \neq 0$) meets with a high potential barrier, which causes a decreasing in their kinetic energies. However, without quintessence ($c = 0$) the particle encounters a low potential barrier, which means that the Dirac particle's kinetic energy would increase.

In Fig. 2, we investigate the behavior of the effective potentials by obtaining potential curves for some specific values of the frequency k while keeping the normalization factor constant ($c = 0.01$). We can see that the potentials have peaks for all values of k. Again, while the frequency increases, the potential barrier increases, and potentials behave similarly in the sufficiently large distances.

The effect of the quintessence term can be observed explicitly by making a three-dimensional plot of the potential with respect to the normalization factor c and the radial distance r. In Fig. 3, we observe a three-dimensional small peak for values of normalization factor c. As the value of radial distances increases, potentials level off. Fig. 4 represents the three-dimensional plot of potential
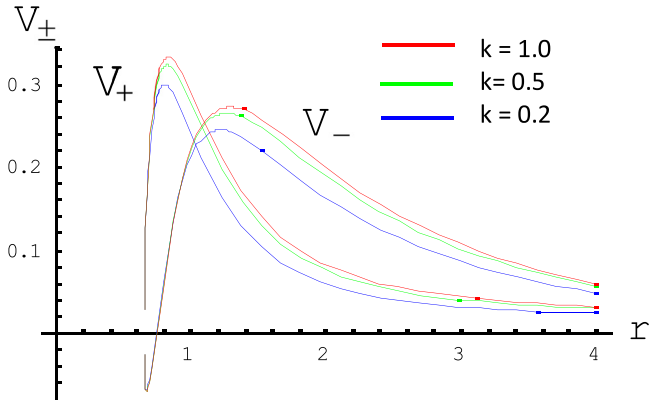
Fig. 2. Family of potential graphs $V_\pm$ for different values of frequency k with $\mu^* = 0.12$, $c = 0.01$, $M = 0.5$, $\lambda = 1$, $\beta = 0.25$, and $w_q = -1$.
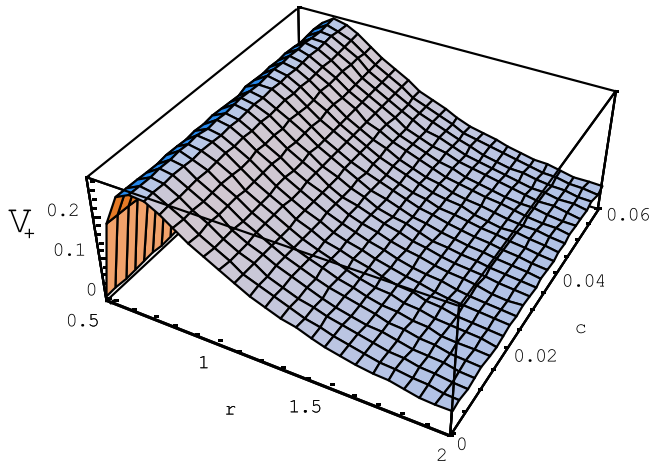

Fig. 3. Three-dimensional plots of potential graphs V_+ for different values of c with $\mu^* = 0.12$, $M = 1$, $k = 0.4$, $\lambda = 0.4$, $\beta = 0.25$, and $w_q = -\frac{1}{3}$.

with respect to frequency k and the radial distance. It is seen from Fig. 4 that; sharp peaks are clear for high frequencies. The effect of the monopole charge of a self-gravitating magnetic field β on the potentials for the massive charged spin-$\frac{1}{2}$ particle can be observed in Fig. 5. We deduce that; high potential barriers are observed for small values of β whereas for large values the potential barriers decrease. Again, the potential levels decrease for large values of distance r and asymptote behavior is manifested. Finally, the three-dimensional plot of potential with varying the state parameter w_q is shown in Fig. 6. We see from Fig. 6 that the potential levels are constant for different values of w_q which implies that the state parameter w_q does not affect the potentials.

5. Greybody radiation of Bosons from BBHSQ

In this section, we evaluate the greybody factor of BBHSQ for spin-0 particles. For the sake of simplicity, we consider the massless Klein-Gordon equation [67]
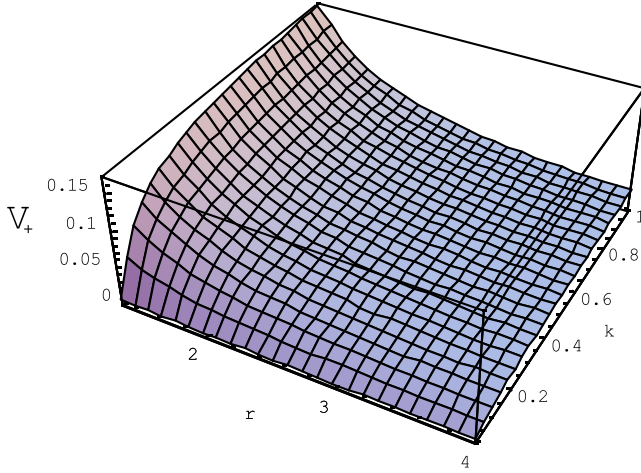
$$\Box \Psi(t, r, \theta, \phi) = 0, \tag{51}$$

Fig. 4. Three-dimensional plots of potential graphs V_+ for different values of k with $\mu^* = 0.12$, $M = 1$, $c = 0.05$, $\lambda = 0.4$, $\beta = 0.25$, and $w_q = -1$.
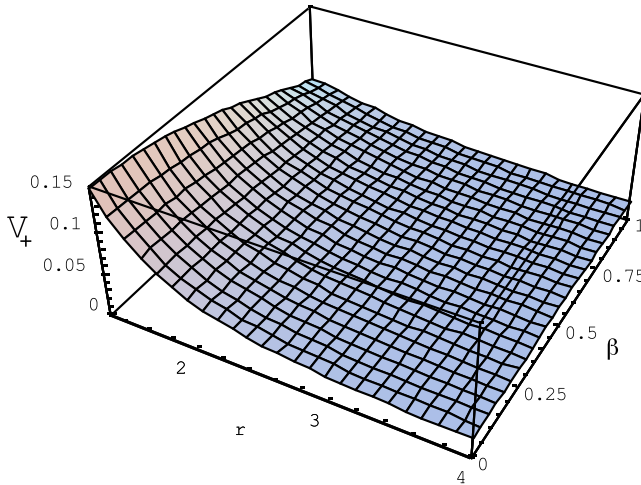

Fig. 5. Three-dimensional plots of potential graphs V_+ for different values of β with $\mu^* = 0.12$, $M = 1$, $c = 0.05$, $\lambda = 0.4$, $k = 0.4$, and $w_q = -\frac{1}{3}$.

where the box symbol denotes the Laplacian operator [68]:

$$\Box = \frac{1}{\sqrt{-g}} \partial_\mu \sqrt{-g} g^{\mu\nu} \partial_\nu. \tag{52}$$

By considering the metric (3) of BBHSQ, then (51) reads

$$-f^{-1}\partial_t^2 \Psi + r^{-2}\partial_r \left(r^2 f \partial_r\right) \Psi + \frac{r^{-2}}{\sin\theta} \partial_\theta \left(\sin\theta \partial_\theta\right) \Psi + \frac{r^{-2}}{\sin^2\theta} \partial_\phi^2 \Psi = 0. \tag{53}$$

Where the scalar field can be defined as

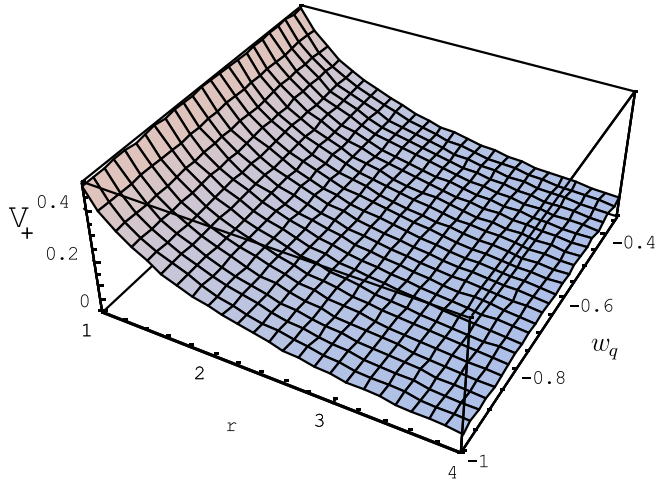$$\Psi = p(r) A(\theta) \exp(-i\omega t) \exp(im\phi), \tag{54}$$

Fig. 6. Three-dimensional plots of potential graphs V_+ for different values of w_q with $\mu^* = 0.12$, $M = 1$, $c = 0.05$, $\lambda = 0.4$, $k = 0.4$, and $\beta = 0.25$.

here ω denotes the frequency of the wave. Substituting the scalar field in (53), one obtains

$$\frac{d^2 p(r)}{dr^2} + \left(f^{-1} \frac{df}{dr} + 2r^{-1} \right) \frac{dp(r)}{dr} + \left(\omega^2 f^{-2} - \widehat{\lambda} r^{-2} f^{-1} \right) p(r) = 0, \tag{55}$$

where $\widehat{\lambda} = l(l+1)$ is the eigenvalue coming from the physical solution of the angular equation of $A(\theta)$, which is nothing but the standard spherical harmonics [60–62]. By changing the variable in a new form as $p = \frac{u}{r}$, the radial wave equation (55) recasts into a one dimensional Schrödinger like equation as follows

$$\frac{d^2 u}{dr_*^2} + \left(\omega^2 - V_{\text{eff}} \right) u = 0, \tag{56}$$

where the effective potential for BBHSQ is given by

$$V_{\text{eff}} = f \left(\frac{\lambda}{r^2} + \frac{1}{r} \frac{df}{dr} \right). \tag{57}$$

To evaluate the greybody factor we use [59,69]

$$\sigma_l(\omega) \geq \sec h^2 \left(\int_{-\infty}^{+\infty} \wp \, dr_* \right), \tag{58}$$

in which r_* is the tortoise coordinate: $\frac{dr_*}{dr} = \frac{1}{f(r)}$, and

$$\wp = \frac{1}{2h} \sqrt{\left(\frac{dh}{dr} \right)^2 + (\omega^2 - V_{\text{eff}} - h^2)^2}. \tag{59}$$

In (59), h is a particular positive function that satisfies the following conditions: $h(r_*) > 0$ and $h(-\infty) = h(\infty) = \omega$ [70]. Here, without loss of generality, we simply set it as $h = \omega$ [69,70], resulting in that the integration of (58) becomes

$$\sigma_l(\omega) \geq \sec h^2 \frac{1}{2\omega} \int_{r_h}^{+\infty} \left(\frac{\lambda}{r^2} + \frac{1}{r} \frac{df}{dr} \right) dr. \tag{60}$$
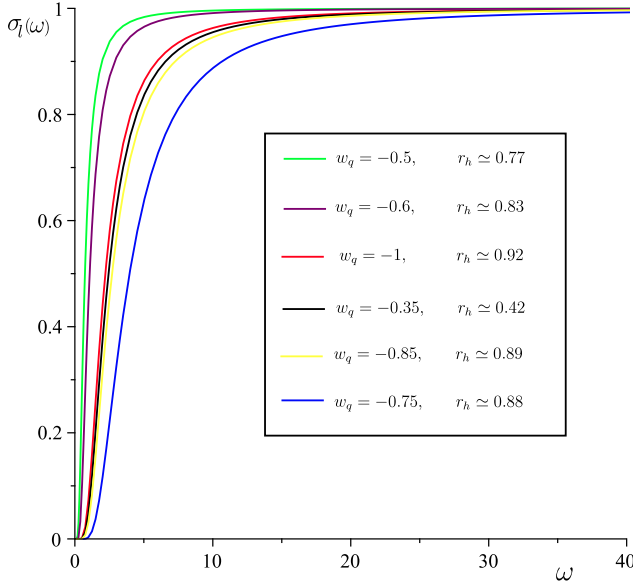
Fig. 7. $\sigma_l(\omega)$ versus ω graph. The plots are governed by Eq. (61). For different w_q values, the corresponding event horizons (i.e, $f(r_h) = 0$) are illustrated. The physical parameters for this plot are chosen as $M = l = c = 1$, and $\beta = 2$.

After making a straightforward calculation, one finds

$$\sigma_l(\omega) \geq \sec h^2 \left(\frac{1}{2\omega} \left[\frac{l(l+1)}{r_h} + \frac{c(3w_q+1)}{(3w_q+2)r_h^{3w_q+2}} - \frac{2M}{\beta^2} + \frac{2M}{\beta^2 \sqrt{1+\frac{\beta^2}{r_h^2}}} \right. \right.$$

$$\left. \left. + \frac{2M}{r_h^2 \left(1+\frac{\beta^2}{r_h^2}\right)^{3/2}} \right] \right), \tag{61}$$

where r_h represents the event horizon.

We depict the greybody factors of the BBHSQ in Fig. 7. As seen from Fig. 7, the values of w_q and event horizon (r_h) are linearly proportional to each other. It is obvious that greybody radiation strictly depends also on the state parameter w_q. According to the information we obtained from the graph, a similar radiation emission occurs around critical w_q values ($-\frac{1}{3}$ and -1). However, while w_q value moves away from those critical values, then radiation may decrease or increase depending on w_q.

6. Greybody radiation of fermions from BBHSQ

In this section, we shall derive the fermionic greybody factors of the neutrinos emitted from BBHSQ. To this end, we consider the case of $w_q = -\frac{1}{3}$ in order to obtain analytical results from Eq. (58). In the case of $w_q = -\frac{1}{3}$, the potentials (45) can be rewritten as

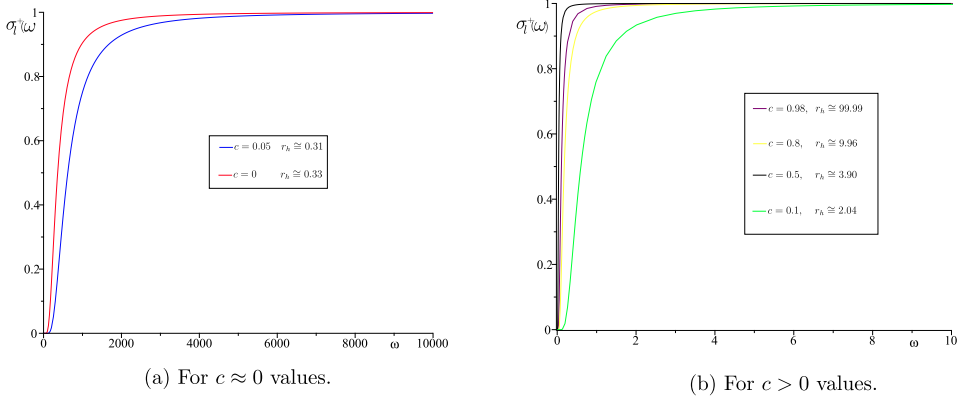$$V_\pm = \frac{\lambda}{r^2}f \pm \frac{\lambda(r-M)}{r^3}\sqrt{f} \mp \frac{2\lambda}{r^2}f^{3/2}, \tag{62}$$

(a) For $c \approx 0$ values.   (b) For $c > 0$ values.

Fig. 8. $\sigma_l^+ (\omega)$ versus ω graph for the case of $w_q = -\frac{1}{3}$. The plots are governed by Eq. (65). For different c values, the corresponding event horizons (i.e, $f(r_h) = 0$) are illustrated. The physical parameters for these plots are chosen as $M = l = 1$, and $\beta = 0.5$.

in which

$$f = 1 - \frac{2Mr^2}{\left(r^2 + \beta^2\right)^{3/2}} - c. \tag{63}$$

Following the procedure described in the previous section [see Eqs. (58)–(62)], one can get

$$\sigma_l^\pm (\omega) \geq \sec h^2 \left(\frac{1}{2\omega} \int_{r_h}^{+\infty} \left[\frac{\lambda}{r^2} \pm \left(\frac{\lambda}{r^2} - \frac{\lambda M}{r^3} \right) \frac{1}{\sqrt{f}} \mp \frac{2\lambda}{r^2} \sqrt{f} \right] dr \right), \tag{64}$$

in which $\sigma_l^+ (\omega)$ and $\sigma_l^- (\omega)$ stand for the greybody factors of the spin-up and spin-down fermions, respectively. After performing some tedious computations, the greybody factors of the fermions can be obtained as follows

$$
\begin{aligned}
\sigma_l^\pm (\omega) \geq \sec h^2 \Bigg\{ \frac{1}{2\omega} \Bigg[\frac{\lambda}{r} &\pm \Bigg(\frac{\lambda}{r_h \sqrt{1-c}} + \frac{M\lambda}{2\,(1-c)^{3/2}\, r_h^2} + \frac{M^2 \lambda}{2\,(1-c)^{5/2}\, r_h^3} + \\
&\frac{-3\lambda M \beta^2 (1-c)^2 + 5M^3 \lambda}{8 r_h^4 (1-c)^3 \sqrt{1-c}} + \frac{-9M^2 \beta^2 \lambda (1-c)^2 + \frac{35}{4} M^4 \lambda}{10 r_h^5 (1-c)^4 \sqrt{1-c}} \\
&- \frac{\lambda M}{2 \sqrt{1-c}\, r_h^2} - \frac{\lambda M^2}{3\,(1-c)^{3/2}\, r_h^3} - \\
&\frac{3\lambda M^3}{8 r_h^4 (1-c)^{5/2}} - \frac{-3\lambda M^2 \beta^2 (1-c)^2 + 5\lambda M^4}{10 r_h^5 (1-c)^3 \sqrt{1-c}} - \frac{-9\lambda M^3 \beta^2 (1-c)^2 + \frac{35}{4} \lambda M^5}{12 r_h^6 (1-c)^4 \sqrt{1-c}} \Bigg) \\
&\mp \Bigg(\frac{2\lambda \sqrt{1-c}}{r_h} - \frac{\lambda M}{\sqrt{1-c}\, r_h^2} - \frac{\lambda M^2}{3\,(1-c)^{3/2}\, r_h^3} + \frac{\lambda \sqrt{1-c}\,\left(3M\beta^2 (1-c)^2 - M^3\right)}{4 r_h^4 (1-c)^3} \\
&+ \frac{\lambda \sqrt{1-c}\,\left(12M^2 \beta^2 (1-c)^2 - 5M^4\right)}{20 r_h^5 (1-c)^4} \Bigg) \Bigg] \Bigg\} \quad (\text{for } 0 \leq c < 1), \tag{65}
\end{aligned}
$$

As it can been seen from Figs. 8 and 9, the greybody factors of spin-up and spin-down fermions exhibit almost the same behaviors as c changes.
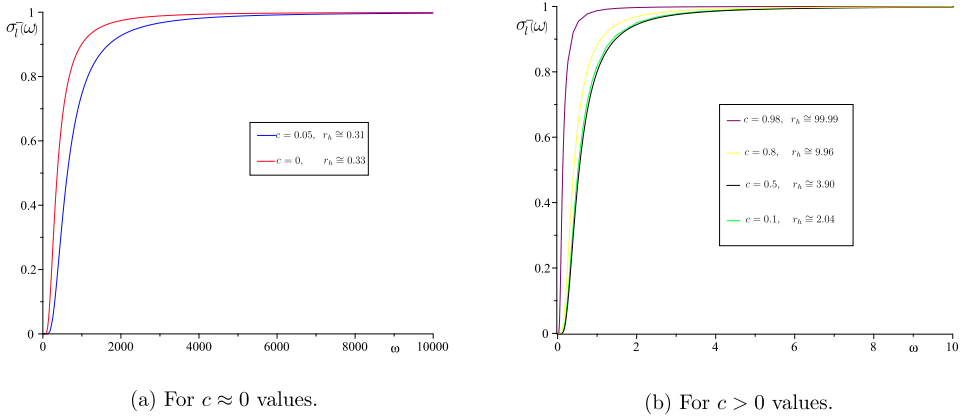
(a) For $c \approx 0$ values.

(b) For $c > 0$ values.

Fig. 9. $\sigma_l^-(\omega)$ versus ω graph for the case of $w_q = -\frac{1}{3}$. The plots are governed by Eq. (65). For different c values, the corresponding event horizons (i.e, $f(r_h) = 0$) are illustrated. The physical parameters for these plots are chosen as $M = l = 1$, and $\beta = 0.5$.

7. Conclusion

In this paper, we have investigated the exact solutions of the Dirac equations that describe a massive, non-charged particle with spin-$\frac{1}{2}$ in the curved space–time geometry of BBHSQ, using NP (null tetrad) formalism. By employing an axially symmetric ansatz for the Dirac spinors, we decouple equations into angular and radial parts. The angular equation leads to the spin-weighted spheroidal harmonics with eigenvalue $\lambda^2 = \left(l + \frac{1}{2}\right)^2$. The radial equations were reduced to pair of one-dimensional Schrodinger-like wave equations with effective potentials for the Dirac particle. We then studied the potentials by plotting them as a function of radial distance. Thus, the effect of the quintessence term on the BBH is unfolded. We revealed that potentials barriers having quintessence matter become more higher than the potentials without the quintessence. We also showed that, as the frequency increases, potentials levels increase as well. However, as the magnetic monopole charge parameter β increases, the potential levels decrease whereas the potentials do not change for varying the state parameter w_q. Remarkably, we depicted how the greybody factors of bosons and fermions vary with the quintessence state parameters w_q (see Fig. 7) and c (see Figs. 8 and 9), respectively.

In future work, we will extend our analysis to the Dirac equation of charged massive fermionic waves propagating in the rotating geometry of the BBHSQ. In this way, we plan to analyze the effect of quintessence on the stationary spacetimes using fermions. For this purpose, we shall also consider the Janis-Newman algorithm [71] for the static BBHSQ (3).

References

[1] P.J.E. Peebles, B. Ratra, Rev. Modern Phys. 75 (2003) 559.
[2] P.A. Ade, et al., Astron. Astrophys. 571 (2014) A1.
[3] R. Caldwell, Braz. J. Phys. 30 (2000) 215.
[4] J.A.S. Lima, Braz. J. Phys. 34 (1A) (2004) 194.
[5] S. Perlmutter, et al., Astrophys. J. 517 (1999) 565.
[6] A.G. Riess, et al., Astron. J. 116 (1998) 1009.
[7] P.M. Garnavich, et al., Astrophys. J. 509 (1998) 74.
[8] V.V. Kiselev, Classical Quantum Gravity 20 (2003) 1187.
[9] Z. Shuang-Yong, Phys. Lett. B 660 (2008) 7.
[10] C. Wetterich, Nuclear Phys. B 302 (1988) 668.
[11] B. Ratra, P.J.E. Peebles, Phys. Rev. D 37 (1988) 3406.
[12] R.R. Caldwell, R. Dave, P.J. Steinhardt, Phys. Rev. Lett. 80 (1998) 1582.
[13] C. Armendariz-Picon, V. Mukhanov, P.J. Steinhardt, Phys. Rev. Lett. 85 (2000) 4438.

[14] C. Armendariz-Picon, V. Mukhanov, P.J. Steinhardt, Phys. Rev. D 63 (2001) 103510.
[15] T. Chiba, T. Okabe, M. Yamaguchi, Phys. Rev. D 62 (2000) 023511.
[16] A.E. Schulz, M. White, Phys. Rev. D 64 (2001) 043514.
[17] R.R. Caldwell, Phys. Lett. B 545 (2002) 23.
[18] S. Nojiri, S.D. Odintsov, Phys. Lett. B 562 (2003) 147.
[19] P. Singh, M. Sami, N. Dadhich, Phys. Rev. D 68 (2003) 023522.
[20] L.P. Chimento, R. Lazkoz, Phys. Rev. Lett. 91 (2003) 211301.
[21] T. Chiba, T. Okabe, M. Yamaguchi, Phys. Rev. D 62 (2000) 023511.
[22] R.J. Scherrer, Phys. Rev. Lett. 93 (2004) 011301.
[23] Z.K. Guo, Y.-S. Piao, X. Zhang, Y.Z. Zhang, Phys. Lett. B 608 (2005) 177.
[24] J.-Q. Xia, B. Feng, X. Zhang, Phys. Rev. D 74 (2006) 123503.
[25] J.M. Bardeen, Non-singular general-relativistic gravitational collapse, in: Proceedings of GR5, Tiflis, Georgia, U.S.S.R., 1968, p. 174.
[26] A. Borde, Phys. Rev. D 50 (1994) 3692.
[27] A. Borde, Phys. Rev. D 55 (1997) 7615.
[28] C. Barrabes, V.P. Frolov, Phys. Rev. D 53 (1996) 3215.
[29] A. Cabo, E. Ayon-Beato, Int. J. Geom. Methods Mod. Phys. A 14 (1999) 2013.
[30] S.A. Hayward, Phys. Rev. Lett. 96 (2006) 031103.
[31] E. Ayon-Beato, A. Garcia, Phys. Rev. Lett. 80 (1998) 5056.
[32] E. Ayon-Beato, A. Garcia, Phys. Lett. B 464 (1999) 25.
[33] E. Ayon-Beato, A. Garcia, Gen. Relativity Gravitation 37 (2005) 635.
[34] M.S. Ma, Ann. Phys. (Amsterdam) 362 (2015) 529.
[35] E. Ayon-Beato, A. Garcia, Phys. Lett. B 493 (2000) 149.
[36] Z.Y. Fan, X. Wang, Phys. Rev. D 94 (2016) 124027.
[37] E. Ayen-Beato, A. Garcia, Gen. Relativity Gravitation 31 (1999) 629.
[38] C. Bambi, L. Modesto, Phys. Lett. B 721 (2013) 329.
[39] B. Toshmatov, Z. Stuchlík, B. Ahmedov, Eur. Phys. J. Plus 132 (2017) 98.
[40] S.G. Ghosh, Eur. Phys. J. C 76 (2016) 1.
[41] K. Ghaderi, B. Malakolkalami, Astrophys. Space Sci. 361 (2016) 161.
[42] B. Mukhopadhyay, Classical Quantum Gravity 17 (2000) 2017.
[43] A. Zecca, Internat. J. Theoret. Phys. 45 (2006) 12.
[44] H. Cebeci, N. Ozdemir, Classical Quantum Gravity 30 (2013) 175005.
[45] T. Birkandan, M. Hortacsu, J. Math. Phys. 48 (2007) 092301.
[46] A. Al-Badawi, I. Sakalli, J. Math. Phys. 49 (2008) 052501.
[47] A. Al-Badawi, Gen. Relativity Gravitation 50 (2018) 16.
[48] A. Al-Badawi, M.Q. Owaidat, Gen. Relativity Gravitation 49 (2017) 110.
[49] C.A. Sporea, Modern Phys. Lett. A 30 (2015) 1550145.
[50] I.I. Cotaescu, Phys. Rev. D 60 (1999) 124006.
[51] I.I. Cotaescu, Phys. Rev. D 65 (2002) 084008.
[52] I.I. Cotaescu, C. Crucean, Modern Phys. Lett. A 22 (2008) 3707.
[53] I.I. Cotaescu, R. Racoceanu, C. Crucean, Modern Phys. Lett. A 21 (2006) 1313.
[54] Y.S. Myung, H.W. Lee, Classical Quantum Gravity 20 (2003) 3533.
[55] T. Harmark, J. Natario, R. Schiappa, Adv. Theor. Math. Phys. 14 (2010) 727.
[56] I. Sakalli, O.A. Aslan, Astropart. Phys. 74 (2016) 73.
[57] H. Gursel, I. Sakalli, Adv. High Energy Phys. 2018 (2018) 8504894.
[58] P. Gaete, I. Schmidt, Internat. J. Modern Phys. A 19 (2004) 3427.
[59] S. Chandrasekhar, The Mathematical Theory of Black Holes, Clarendon, London, 1983.
[60] E.T. Newman, R. Penrose, J. Math. Phys. 3 (1962) 566.
[61] S.K. Chakrabarti, Proc. R. Soc. Lond. Ser. A Math. Phys. Eng. Sci. 391 (1984) 27.
[62] J.N. Goldberg, A.J. Macfarlane, E.T. Newman, F. Rohrlich, E.C.G. Sudarsan, J. Math. Phys. 8 (1967) 2155.
[63] A.M. Davydov, Quantum Mechanics, second ed., Oxford, Pergamon, 1976.
[64] J. Mathews, R.L. Walker, Mathematical Methods of Physics, second ed., W.A. Benjamin, New York, 1970.
[65] K. Ghaderi, B. Malakolkalami, Nuclear Phys. B 903 (2016) 10.
[66] S. Mahamat, B.B. Thomas, Eur. Phys. J. C 78 (2018) 325.
[67] R.M. Wald, General Relativity, The University of Chicago Press, Chicago and London, 1984.
[68] S.H. Mazharimousavi, I. Sakalli, M. Halilsoy, Phys. Lett. B 672 (2009) 177.
[69] S. Kanzi, I. Sakalli, Nucl. Phys. B, arXiv:1905.00477 (in press).
[70] Y.G. Miao, Z.M. Xu, Phys. Lett. B 772 (2017) 542.
[71] H. Erbin, Universe 3 (2017) 19.